

**SPARC-BD-03/003**  
**LNF-03/06 (P)**  
**5 Maggio 2003**

## **RECENT ADVANCES AND NOVEL IDEAS FOR HIGH BRIGHTNESS ELECTRON BEAM PRODUCTION BASED ON PHOTO-INJECTORS**

M. Ferrario<sup>1</sup>, M. Boscolo<sup>1</sup>, V. Fusco<sup>1</sup>, C. Vaccarezza<sup>1</sup>,  
C. Ronsivalle<sup>2</sup>, J. B. Rosenzweig<sup>3</sup>, L. Serafini<sup>4</sup>.

- <sup>1</sup>*INFN-Laboratori Nazionali di Frascati Via E. Fermi 40, I-00044 Frascati, Italy*  
<sup>2</sup>*Ente Nazionale Energie Alternative, Via Enrico Fermi 45, 00044 Frascati (Roma), Italy*  
<sup>3</sup>*UCLA, Dep. of Physics and Astronomy, Los Angeles, CA 90095*  
<sup>4</sup>*INFN-Sezione di Milano, Via Celoria 16, 20133 Milano, Italy*

### **Abstract**

Photo-injectors beam physics remains a fruitful and exciting field of research. New ideas have been recently proposed to achieve ultra-high brightness beams, as particularly needed in SASE-FEL experiments, and to produce flat beams as required in linear colliders. An overview of recent advancements in photo-injector beam physics is reported in this paper.

PACS.: 29.27.Bd

*Invited talk at the ICFA Workshop on  
“The Physics & Applications of High Brightness Electron Beams”  
Chia Laguna, Sardinia, ITALY  
July 1-6, 2002*

## 1 INTRODUCTION

The research and development of high brightness (high current, low emittance) beam production by photo-injectors has been driven in the last decade mainly by self amplified, spontaneous emission, free-electron laser (SASE FEL) applications. Beams with normalized emittances lower than 1  $\mu\text{m}$ , with peak current of some kA, are required for example for the new x-ray SASE FEL projects [1,2]. A revival of longitudinal focusing techniques with a deeper understanding of emittance compensation theory [3] has opened up a new possibility of compressing the beam inside an RF structure or in a downstream drift, with a proper beam control employed through solenoid focusing to avoid the emittance degradation. This option may avoid the serious phase space degradations observed in magnetic chicans caused by coherent synchrotron radiation (CSR) emitted in the bends [4]. Kilo-ampere beams with low emittance have been predicted by simulations for the so-called velocity bunching configuration [5]. At Neptune (UCLA) [6], DUVFEL (BNL) [7] and PLEIADS (LLNL) [8] preliminary experimental results (in non-optimized beam lines) have verified the usefulness of this idea for strongly compressing photoinjector-derived beams, despite the space charge induced emittance degradation observed.

In a different context, a new technique has been recently proposed [9] and tested [10] by a DESY/FNAL collaboration, the so-called flat beam production, which is an important goal for linear colliders. It consists in a simple transformation of a magnetized round beam, with equal emittances in both transverse planes, produced by a photo-cathode embedded in a solenoid field, which is then followed by a skew quadrupoles triplet. With proper matching, a flat beam with high transverse emittance ratio (300) as required by linear colliders, may in principle be obtained. Experimental results have achieved so far an emittance ratio of 50.

An overview of these recent advancements in photo-injector beam physics is given in this paper.

Transverse normalized beam brightness is a quality factor of the beam defined as [11]:

$$B_{\square} = \frac{2I}{\epsilon_{i,x}\epsilon_{i,y}} \quad (1)$$

where  $I$  is the bunch peak current and  $\epsilon_i$  is the rms normalised emittance. The meaning of brightness can be understood by expressing the peak current by the transverse current density  $I=J\epsilon^2$  and the emittance at waist as  $\epsilon_i=\epsilon\epsilon'$  so that taking  $\epsilon_{i,x}=\epsilon_{i,y}$  one obtains:

$$B_{\square} = \frac{2J}{(\epsilon\epsilon')^2} \quad (2)$$

In this way, transverse brightness can be seen as the beam peak current density normalized to the rms beam divergence angle, i. e. a quality factor of a beam propagating with low divergence and high current density, as required for FEL interaction, or Thomson back-scattering applications.

By examining the SASE FEL scaling laws [12], one can understand the importance of a high brightness beam for achieving short radiation wavelength  $\lambda_r$  with short gain length  $L_g$ :

$$\sigma_r^{min} = \frac{\sigma_r \sqrt{(1 + K^2/2)}}{B_0 K^2} \quad (3)$$

$$L_g = \frac{\sigma^2/2}{K \sqrt{B_0} (1 + K^2/2)} \quad (4)$$

where  $K$  is the undulator parameter.

Another way of viewing the requirements on the beam for FEL applications is through the emittance alone. The coherent part of the radiation from an undulator can be approximately described as an equivalent source at the undulator center [13], where the minimum photon beam phase space area is limited by diffraction and is given by

$$\sigma_{ph} = \sigma_{ph} \sigma'_{ph} = \frac{\sigma_r}{4\sigma}, \quad (5)$$

where  $\sigma_{ph}$  and  $\sigma'_{ph}$  are the source radius and divergence respectively. In this picture the optimum condition during SASE interaction requires phase space matching of electron and photon beams in both transverse planes;

$$\sigma_{i,x} = \sigma_{i,y} \sigma_{ph}, \quad (6)$$

a condition that allows to operate in the round beam configuration with  $\sigma_{i,x} = \sigma_{i,y}$ .

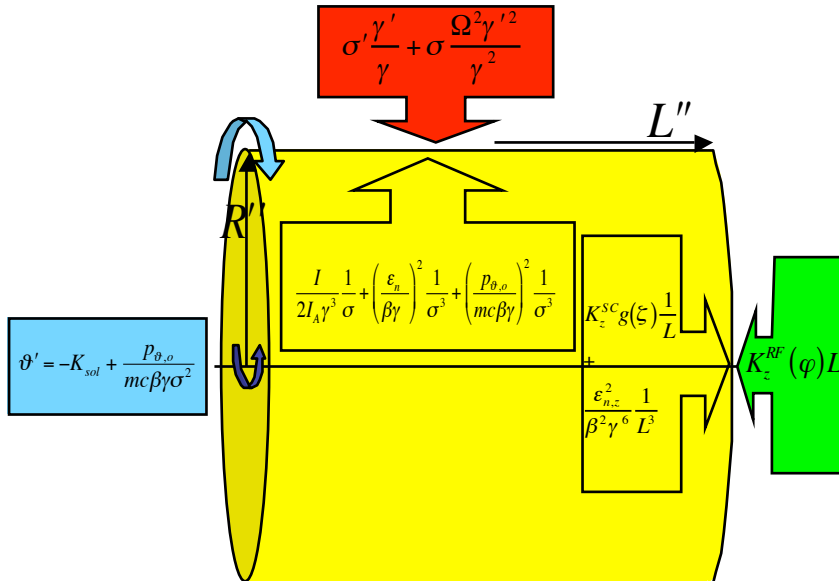


**FIG. 1:** A schematic representation of the envelope equations [14] describing the dynamics of a beam subject to its self field and external fields.

We now discuss the factors affecting the propagation and manipulation of the electron beams needed for advanced applications. As shown in Fig. 1, a high brightness electron beam is subject to transverse defocusing forces originated by space charge field, by emittance pressure, and by an equivalent emittance terms  $\epsilon_B = p_{\perp,o}/mc$  accounting for the centrifugal potential when the canonical momentum  $p_{\perp}$  is different from zero.

The defocusing forces on the beam can be counteracted by external fields like solenoids, and alternating gradient transverse component of RF accelerating fields. Additionally, transverse motion is naturally damped by acceleration. Similarly, along the longitudinal axis defocusing forces are generated by space charge and longitudinal emittance, while a proper phasing of the RF field can be used to produce longitudinal focusing. The beam may also rotate inside a solenoid field and, in a more complicated way, also in a quadrupole channel. Rotation can be balanced or properly tuned as a consequence of the conservation of canonical angular momentum, when the beam is generated in a gun embedded in a solenoid field.

High brightness beams experience two distinct regimes along the accelerator, depending on the laminarity parameter (the ratio between the space charge term and the emittance term in the transverse envelope equation):

$$\epsilon = \frac{I\epsilon^2}{2\epsilon_A(\epsilon_h + \epsilon_B)^2} \quad (7)$$

When  $\epsilon \gg 1$  the transverse beam dynamics are dominated by space charge effects, and the beam propagated in the quasi-laminar regime in which particle trajectories do not cross each other, as shown in Fig. 2 (left). Correlated emittance oscillations are observed in this regime [3], caused by the different local current along the bunch and by finite bunch length effects. By accelerating the beam, a transition occurs to the so-called emittance dominated regime, when  $\epsilon \ll 1$ , in this case the transverse beam dynamics are dominated by the emittance and trajectories are not parallel anymore, as shown in Fig. 2 (right).

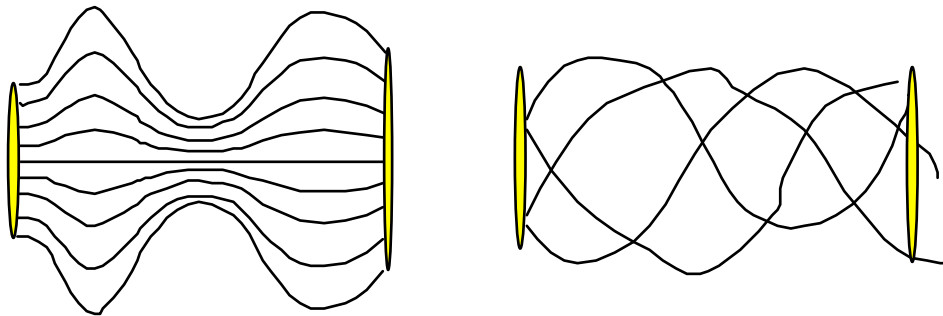


**FIG. 2:** Schematic representation of a quasi-laminar beam trajectories (left plot) and of an emittance dominated beam trajectories (right plot).

In the following sections we describe how a beam can be manipulated in straightforward ways to obtain high brightness in FELs, and the possibility of high luminosity in linear colliders.

## 2 EMITTANCE COMPENSATION: THE CONCEPT OF INVARIANT ENVELOPE AND THE NEW WORKING POINT

In a photo-injector, electrons are emitted by a photo-cathode located inside an RF cavity that is illuminated by a laser pulse, so that the bunch length and shape can be controlled on a picosecond time scale via the properties of the laser pulse [15]. The emitted electrons are rapidly accelerated to relativistic energies, thus partially mitigating the emittance growth due to space charge force effects. Nevertheless the phase dependent focusing forces that the electrons experience in the RF field [16] result in an RF induced emittance growth. In order to keep this effect small the transverse and longitudinal bunch dimensions have to be kept small. The increased particle densities lead, in turn, to increased space charge forces thus partially counteracting the beneficial effects of the high gradients available in RF cavities.

Since the early '80s it was clear that this large space charge-induced emittance growth in an RF gun is partially correlated and can be reduced by a simple focusing scheme first studied by B.Carlsten [17]. The space charge in fact acts to first order as a defocusing lens, the strength of which varies over the bunch length. The force is strongest in the middle slice of the bunch and decreases towards both ends. Therefore a fan-like structure appears in the phase space. After a focusing kick is applied by means of an external solenoid, the fan slices distribution tends to close in the following drift space until a minimum phase space area is reached, corresponding to a partial re-alignment of bunch slices. A residual emittance growth is nevertheless left in practical cases, caused by non-linear space charge fields within the bunch [18] and chromatic effect in the solenoid.

In order to avoid additional space charge emittance growth in the subsequent beam line, the emittance minimum has to be reached at high beam energy so that space charge forces are sufficiently damped. The beam has to be properly matched to the following accelerating sections in order to keep under control emittance oscillations and obtain the required emittance minimum at the injector exit.

A full theoretical description of the emittance compensation process [3] has demonstrated in fact that in the space charge-dominated regime, *i.e.* when the space charge collective force is largely dominant over the emittance pressure, mismatches between the space charge correlated forces and the external focusing gradient produce slice envelope oscillations that cause normalized emittance oscillations. It has been shown that to also damp these emittance oscillations secularly, the beam has to be propagated close to a the so-called invariant envelope, given by

$$\sigma_{INV} = \frac{I}{I_A} \sqrt{\frac{2I}{I_A(1+4\sigma^2)}} \quad (8)$$

where  $\sigma = 1 + T/mc^2$  is the normalized beam kinetic energy while the normalized accelerating gradient is defined by  $\sigma = \frac{eE_{acc}}{m_e c^2} \approx 2E_{acc}$ ,  $E_{acc}$  is the accelerating field,  $I$  is the beam peak current in the bunch, and  $I_A = 17$  kA is the Alfven current. The normalized focusing gradient is defined as:

$$\sigma^2 = \frac{eB_{sol}^2}{mc^2} + \begin{cases} 1/8 & SW \\ 0 & TW \end{cases} \quad (9)$$

for a superposition of magnetic field of solenoids and RF ponderomotive focusing by standing wave or traveling wave sections.

The invariant envelope  $\sigma_{INV}$  is an exact analytical solution of the rms envelope equation for laminar beams:

$$\sigma'' + \sigma \left( \frac{\sigma'}{\sigma} \right)^2 + \sigma \frac{\sigma'^2}{\sigma^2} - \frac{I}{2I_A \sigma^2} = \frac{\sigma_h^2}{\sigma^3} \approx 0 \quad (10)$$

where the thermal emittance term (r.h.s.) is considered negligible. This solution corresponds to a generalized Brillouin flow condition that assures emittance correction, *i.e.* control of emittance oscillations associated with the envelope oscillations such that the final emittance at the photoinjector exit is reduced to an absolute minimum.

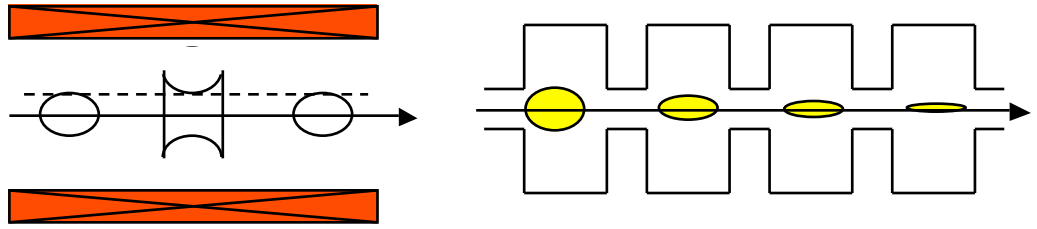


**FIG. 3:** Schematic representation of a Brillouin flow in a drift (left plot) and an invariant envelope in an accelerating structure (right plot).

In order to assure this condition, it is necessary to match two types of flow along the photoinjector (see Fig. 3): the invariant envelope inside accelerating sections and Brillouin flow, given by:

$$\sigma_{BRI} = \frac{mc}{eB_{sol}} \sqrt{\frac{I}{2I_A \sigma}} \quad (11)$$

in intermediate drift spaces.

By substituting the  $\sigma_{INV}$  expression (8) in laminarity parameter definition (7) one can see that the laminar regime extends up to an energy given by:

$$\sigma \approx \sqrt{\frac{2}{3}} \frac{I}{I_A \sigma_h} \quad (12)$$

As a consequence of such a theory, the definition of the “injector” has to be extended up to an energy high enough to exit the laminar regime, as one can see from Fig. 4. The beam enters then in the so called emittance-dominated regime, where trajectories cross over dominates over space charge oscillations and the total normalized emittance remains constant in an ideal accelerator. For example, with the expected SPARC/FEL [19] injector parameters  $I=100$  A,  $E_{acc}=25$  MV/m and an estimated [20] thermal emittance of  $0.3 \mu\text{m}$  for a copper cathode with UV excitation, the transition occurs near 150 MeV.

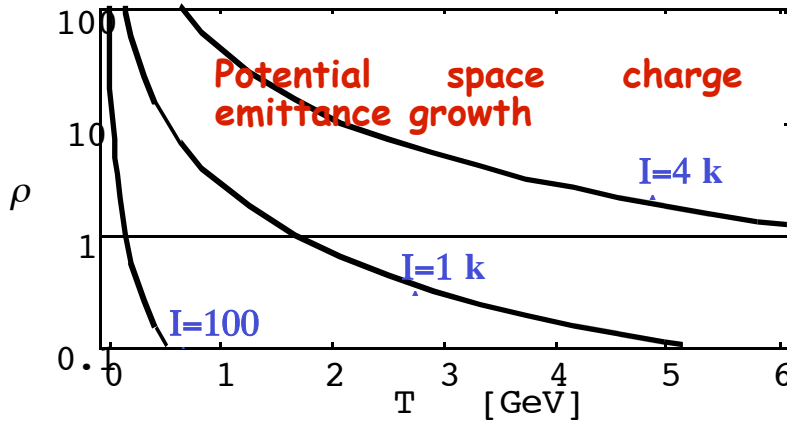


**FIG. 4:** Laminarity parameter  $\bar{\epsilon}$  versus beam energy  $T$  for different beam currents.

Following the given matching condition, a new working point very suitable for damping emittance oscillations has been recently found [21] in the context of the LCLS FEL project [1]. It has been found that the correlated emittance can be damped to the level of  $0.3 \mu\text{m}$  at 150 MeV for a uniform charged cylindrical bunch in this design. The main feature of such an effective working point are described here after.

Let us consider the emittance compensation regime of a space charge-dominated beam downstream the gun cavity of a split RF photo-injector configuration, Fig. 5.

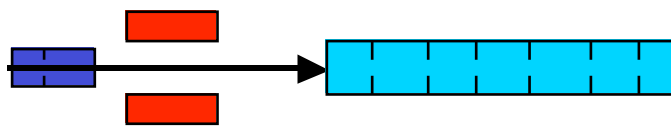


**FIG. 5:** Schematic representation of a split RF photo-injector configuration: 1.6 cells RF gun, solenoid, and accelerating structure.

In the drifting region downstream the gun the emittance evolution displays a double minimum, with the distance between the two minima decreasing with increasing of the solenoid strength.

It has been shown [21] that if the booster is located where the relative emittance maximum and the envelope waist occur, the second emittance minimum can be shifted to the booster exit and frozen at a very low level to the extent that the invariant envelope matching conditions are satisfied, see Fig. 6.

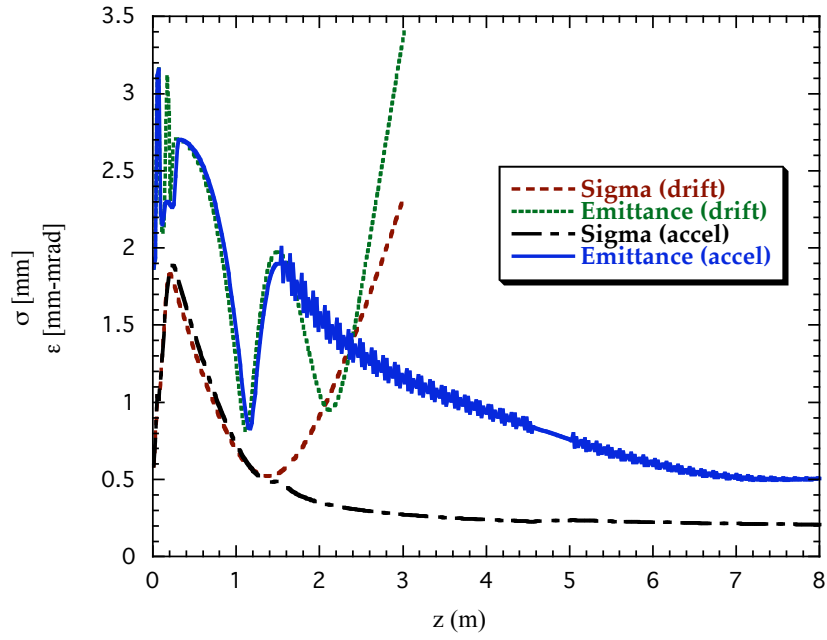


**FIG. 6:** HOMDYN simulation of an optimized split photo-injector. Transverse rms beam size and normalized emittance, with and without booster.

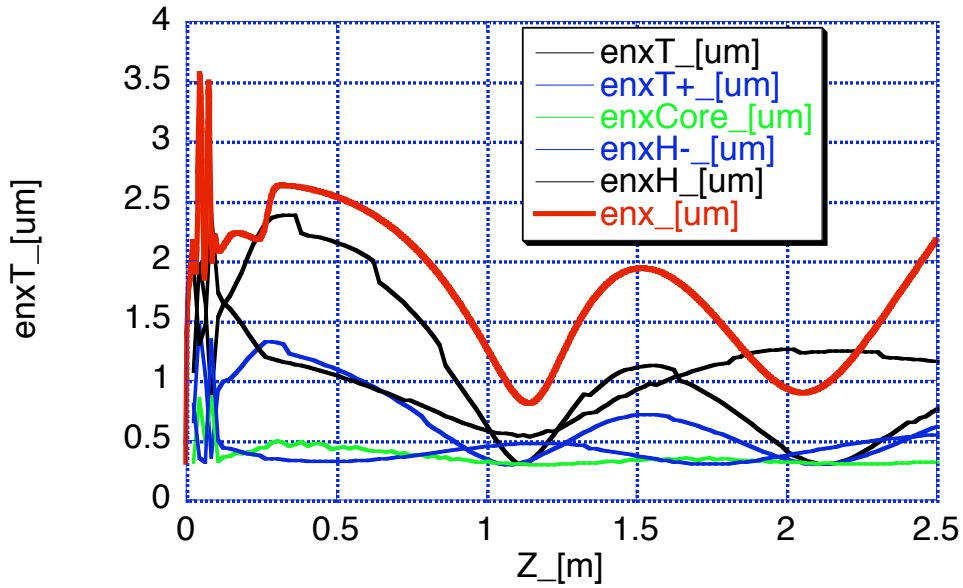


**FIG. 7:** Total rms normalized emittance for an S-band gun with solenoid (red bold line) from the cathode along a 2.3 m long drift, together with the rms normalized emittance computed for five representative 400  $\mu\text{m}$  long slices, located at the longitudinal extrema and in the core of the bunch.

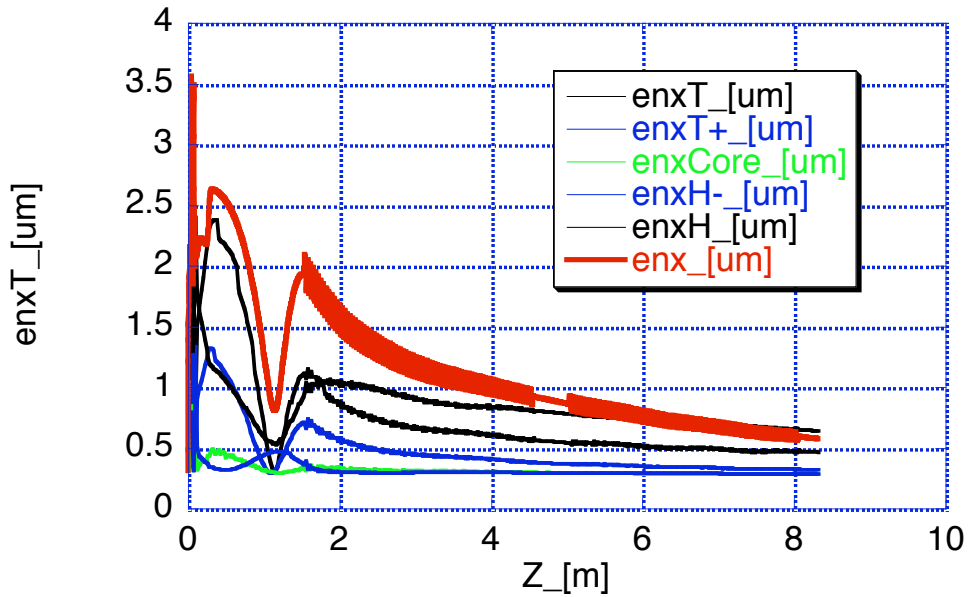


**FIG. 8:** Same as Fig. 7 but with a booster located at  $z=1.5$  m.

A slice analysis shows that the core of the bunch exhibits only minor emittances oscillation (it has very little effective variation of the defocusing space charge force) while the tails experience a noticeable oscillation driving also the total emittance oscillation see Fig. 7 and Fig. 8. The emittance compensation occurring in the booster when the invariant envelope matching conditions are satisfied is actually limited by the head and tail slice behavior; these slices also carry the most pronounced energy deviation, as shown in Fig. 9.

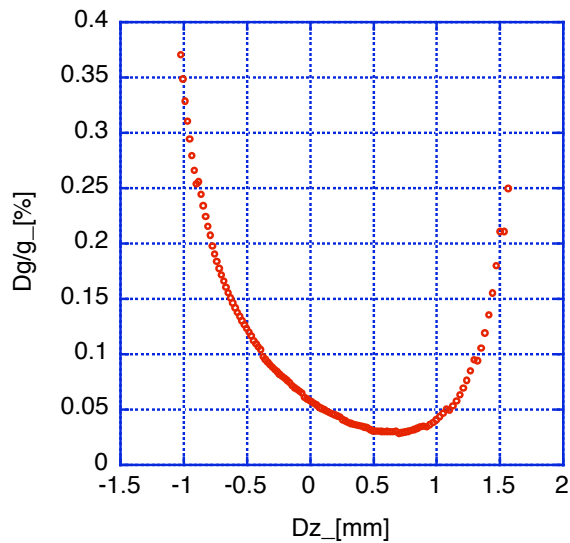


**FIG. 9:** Energy deviation along the bunch at  $z=0.2$  (solenoid centre) computed for a 400  $\mu\text{m}$  long slice centered at  $Dz$ .

The origin of the double emittance minimum downstream of the solenoid location can be explained as mainly due to a chromatic effect occurring inside the solenoid. Following [3], a simple heuristic example helps to understand this process. Let consider a beam traveling in a long solenoid channel without acceleration, subject to its own space charge field and an external focusing force. Such a beam can be described by the following rms envelope equation, neglecting the thermal emittance term:

$$\sigma'' + k^2 \sigma = \frac{I g(\sigma)}{2I_A \sigma^3} \quad (13)$$

where  $k = \frac{eB}{2mc\sigma}$  is the external solenoid parameter (depending on  $L$ ),  $\sigma$  is the coordinate along the bunch and  $g(\sigma)$  is the space charge field form factor, that for a uniform charged cylinder with radius  $R$  and length  $L$  is given by [21]

$$g(\sigma) = \frac{I \sigma / L}{2\sqrt{(I \sigma / L)^2 + A^2}} + \frac{\sigma / L}{2\sqrt{(\sigma / L)^2 + A^2}}, \quad (14)$$

where  $A = \frac{R}{L}$  is the bunch aspect ratio.

An equilibrium solution of Eq. 13 can be easily found by setting  $\sigma'' = 0$ , leading to the already quoted Brillouin flow solution,

$$\sigma_{eq}(\sigma, \sigma) = \sqrt{\frac{I g(\sigma)}{2I_A \sigma^3} \frac{1}{k}}. \quad (15)$$

Notice that each slice along the bunch, identified by its coordinate  $\sigma$ , has a different equilibrium solution, not only because of the  $\sigma$  dependence of the space charge field form factor, that from now on we will assume constant  $g(\sigma) = 1$ , but also because of the  $L$  dependence of the solution. In case of a significant correlated energy spread along a cylindrical uniformly charged bunch with transverse size  $\sigma_c$  (assuming at the beginning each slice has the same  $\sigma_c$ ) only the slice with the correct  $\sigma_b$ , if any, will be in equilibrium with a given external field  $B$ . Any other slice will oscillate around the initial size  $\sigma_c$  according to the solution of the linearized envelope equation about its equilibrium solution (assuming  $\sigma'' = 0$ ),

$$\sigma(z, \sigma, \sigma) = \sigma_{eq}(\sigma, \sigma) + \Delta\sigma(\sigma, \sigma) \cos(\sqrt{2}k(\sigma)z), \quad (16)$$

where  $\Delta\sigma(\sigma, \sigma) = \sigma_c - \sigma_{eq}(\sigma, \sigma)$ , as shown in Fig. 10.

Notice that in this case each slices has its own oscillation amplitude and its own oscillation frequency.

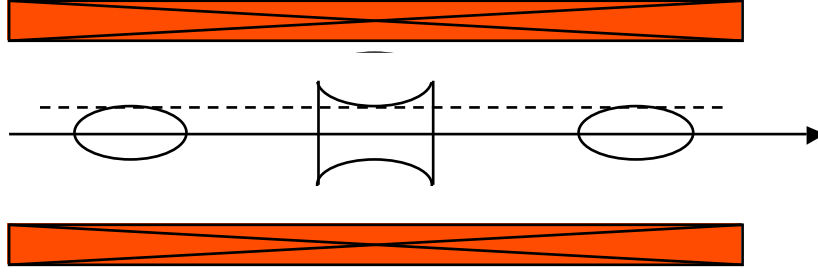


**FIG. 10:** Schematic representation of a Brillouin flow. Notice that only the central slice is in equilibrium, the other slices are oscillating around their own equilibrium solution.

Let us compute now the emittance oscillations of a bunch with a linear energy spread correlation entering in a long solenoid at a waist. Taking into account only two representative slices with a slightly different energy:  $\sigma_+ = \sigma_0(1 + \delta_+)$  and  $\sigma_- = \sigma_0(1 - \delta_-)$ , where  $\delta_{\pm} = \frac{\Delta E_{\pm}}{E_0}$ , a convenient way to calculate the emittance has been described in [22], the rms normalized emittance for a two slice bunch is given by

$$\sigma_i = \frac{\sigma_0}{2} \left| \sigma_+ \sigma_- \left( \sigma_+ \sigma_- \right) \right|. \quad (17)$$

Substituting

$$\begin{aligned} \sigma_+ &= \sigma_{eq+} + \Delta\sigma_+ \cos(\sqrt{2}k_+z) & \sigma_- &= \sigma_{eq-} + \Delta\sigma_- \cos(\sqrt{2}k_-z) \\ \Delta\sigma_+ &= \Delta\sigma_0 \sqrt{2}k_+ \Delta\sigma_+ \sin(\sqrt{2}k_+z) & \Delta\sigma_- &= \Delta\sigma_0 \sqrt{2}k_- \Delta\sigma_- \sin(\sqrt{2}k_-z) \end{aligned} \quad (18)$$

into to (17) one obtains, to first order in  $\delta_{\pm}$ ,

$$\sigma_i = \frac{\sigma_0}{\sqrt{2}} k_0 \left| \sigma_{eq0} \left( 2\Delta\sigma_0 + \delta_+ \right) \sin \left( \frac{\Delta\sigma_0}{2} z \right) \cos(\langle k \rangle z) + \Delta\sigma_0^2 \sin(\Delta\sigma_0 z) \right| \quad (19)$$

where  $\langle k \rangle = \frac{1}{\sqrt{2}}(k_+ + k_-) = \sqrt{2}k_0$  is the average beam plasma frequency,  $\Delta\sigma_0 = \sqrt{2}(k_- - k_+) = 2\sqrt{2}k_0\delta_+$  the modulating plasma frequency and  $\Delta\sigma_0 = \Delta\sigma_c - \Delta\sigma_{eq0}$  is the envelope offset with respect to the nominal energy equilibrium solution. When  $z \ll \frac{\sigma_0}{2\Delta\sigma_0 k}$  Eq. 19 can be approximated by the following expression,

$$\sigma_i = \frac{\sigma_0}{\sqrt{2}} k_0 \Delta\sigma_0 \left| \left( \sigma_{eq0} \left( 2\Delta\sigma_0 + \delta_+ \right) \cos(\langle k \rangle z) + \Delta\sigma_0 \right) \Delta\sigma_0 z \right|. \quad (20)$$

In Fig. 11, the average envelope (Eq. 18) and emittance oscillations predicted by Eq. 19 are reported, and these qualitatively reproduce the double emittance minimum behavior around seen in the more complex photoinjector case discussed above.

When the initial envelope offset is not too far from the equilibrium solution (Eq. 15), the emittance oscillates with the average plasma frequency and periodically goes back to its initial value. By increasing the initial envelope offset the emittance evolution is dominated by the beating term and the original minimum is recovered only after a longer period, as shown in Fig. 12. This is a warning for beam operation in long solenoid devices in which the beam current varies, as will be discussed in the next section.

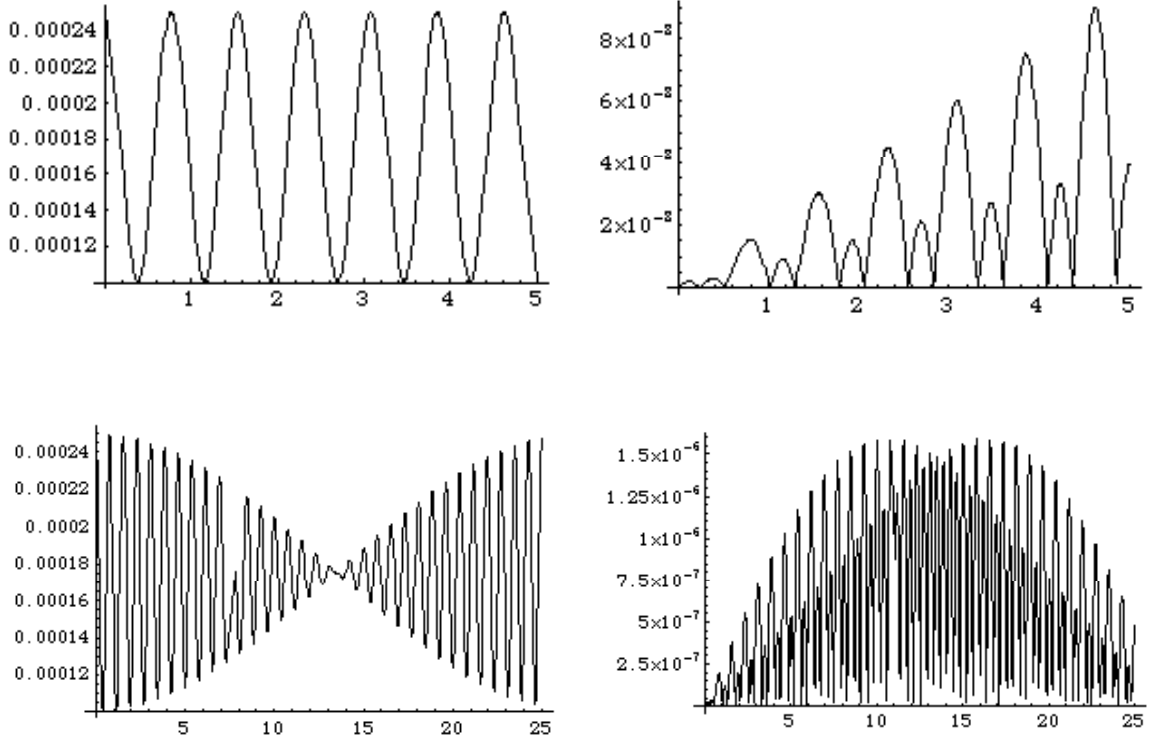


**FIG. 11:** Envelope (left) and normalized emittance (right) evolution, as predicted by Eq. 19, reproducing the behavior of Fig. 7. Lower plots show a longer propagation length scales

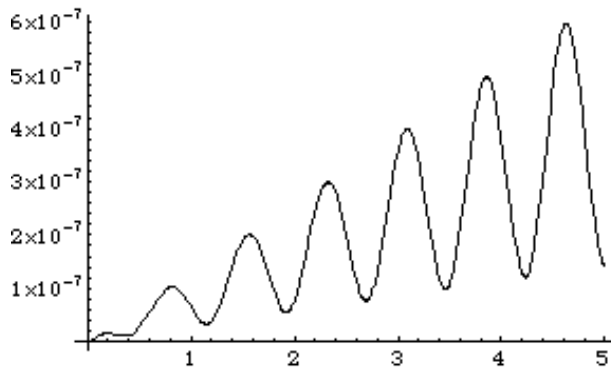


**FIG. 12:** Normalized emittance as predicted by Eq. 19 with  $\square_c=3\square_{eq0}$

This working point has been easily scaled to different gun RF frequency and bunch charge design through well-known techniques [23]. It might also be convenient to operate the injector at a different gradient with respect to the original design, while keeping the beam line unchanged. In

this case the scaling has to preserve the main feature of the original bunch in terms of average and beating plasma frequencies. A reduced gun peak field results in a lower energy gain, hence a first scaling law can be deduced by the condition of keeping the average plasma frequency invariant,

$$B \propto \langle \Delta \rangle. \quad (21)$$

The beating plasma frequency is related to the relative energy spread along the bunch. The longitudinal phase space in the center of the solenoid ( $z=0.2$  m) is shown in Fig. 13.

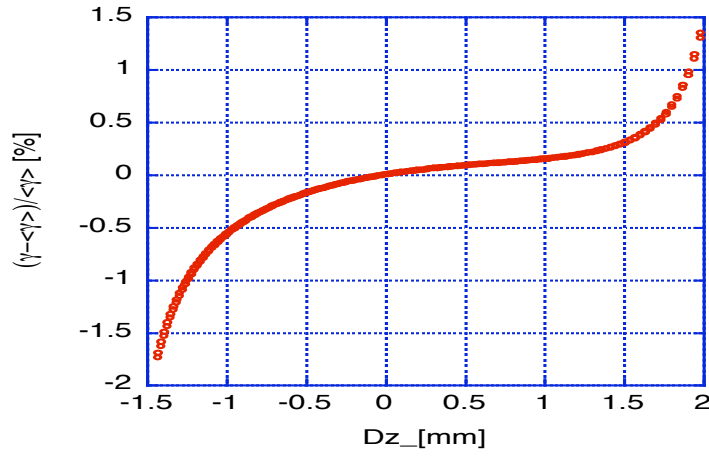


**FIG. 13:** Longitudinal phase space in the center of the solenoid ( $z=0.2$  m).

As one may easily note the energy correlation is dominated by a third order longitudinal correlation typical of the longitudinal space charge-induced energy spread. To keep such a correlation one has to keep unchanged the beam aspect ratio  $A$ , resulting in

$$\frac{\sigma_r}{\sigma_l} \propto \langle \Delta \rangle, \quad (22)$$

and the current density  $J \propto Q/\sigma_l \sigma_r^2$  scales like [23]

$$J \propto \langle \Delta \rangle^3. \quad (23)$$

For a constant charge scaling, Eqs. 22 and 23 taken together imply that  $\sigma_l \propto \langle \Delta \rangle^{5/3}$  and  $\sigma_r \propto \langle \Delta \rangle^{2/3}$ .

For example scaling the original bunch parameters  $R=1$  mm,  $L=10$  ps and solenoid  $B=0.31$  T, to operation with reduced gun peak field, from 140 MV/m to 120 MV/m, one obtains  $R=1.1$  mm,  $L=12.7$  ps and  $B=0.27$  T. The original, unscaled (continuous line) and scaled (dashed line) envelopes and emittances are shown in Fig. 14. This comparison seems to indicate that our scaling considerations work quite well.

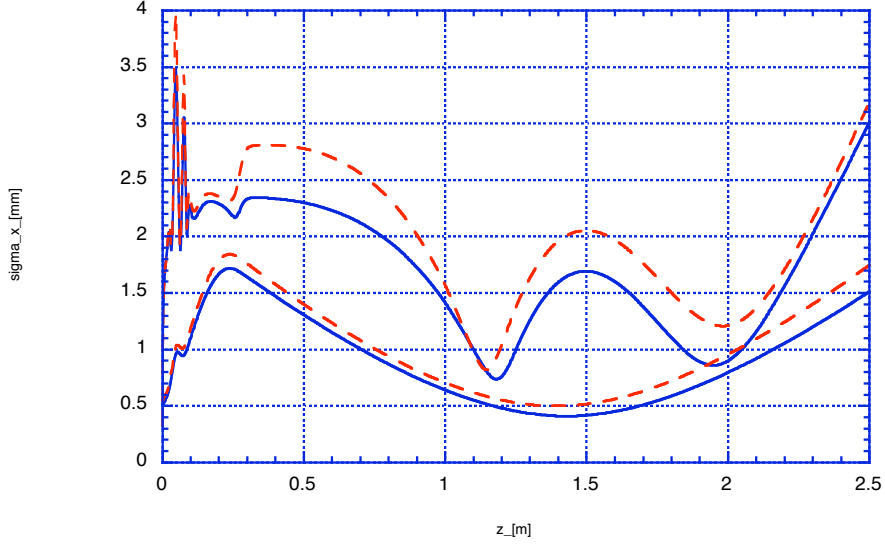


**FIG. 14:** Original (continuous line) and scaled (dashed line) envelopes and emittances

The theory of the invariant envelope has been a very important tool to clarify the emittance compensation process. In the next section we discuss how the concepts introduced in this section can be extended to the case of a bunch under the effect of a longitudinal focusing.

### 3 HIGH PEAK CURRENT: THE CONCEPT OF VELOCITY BUNCHING

Since the impact of magnetic compressors on the beam quality is a relevant and compelling topic, with the tendency to have serious emittance growth due to coherent synchrotron radiation effects in bends [4], a new method able to compress the bunch at moderate energies (tens of MeV), using rectilinear trajectories, and integrated in the emittance compensation process described in the previous section, has been recently proposed [5]. The so-called velocity bunching scheme is based on the weak synchrotron motion that the electron beam still undergoes at low energies in the RF wave of linear accelerating structures.

This combined bunching and emittance control technique has been extensively explored by numerical simulation studies of the entire photo-injector system that generates the ultra-short electron bunches, up to an energy 150 MeV. Additionally, recently the first experimental confirmations of the simulation and theoretical predictions have been observed at a number of laboratories [6,7,8]. Other experiments in the past showed some evidence of this process [24]. The promise is to attain 10-100 fs long bunches with charges ranging from 10 pC up to a few nC.

Before discussing this technique in detail, let us recall that rectilinear bunching techniques have been applied extensively in the past, both in the field of thermo-ionic injectors and also in photo-injectors. The previously explored schemes are all based on inducing an energy chirp on a moderately relativistic beam (say a few MeV, by running it through a RF cavity far off crest) and letting it drifting in free space to turn the energy correlated chirp into a rotation of the

longitudinal phase space distribution, hence a compression of the bunch. Therefore the peak current is increased, leading to strong space charge effects caused by the increase of phase space density occurring at a constant energy. We will name this well-known technique "*ballistic bunching*", to emphasize to the mainly ballistic behavior of the applied phase space manipulation in free space.

The scheme we refer to as *velocity bunching* has the following characteristics: although the phase space rotation in this process is still based on a correlated velocity chirp in the electron bunch, in such a way that electrons on the tail of the bunch are faster (more energetic) than electrons in the bunch head, this rotation does not happen in free space but inside the longitudinal potential of a traveling RF wave which accelerates the beam inside a long multi-cell traveling wave (TW) RF structure, applying at the same time an off crest energy chirp to the injected beam. This is possible if the injected beam is slightly slower than the phase velocity of the RF wave so that, when injected at the crossing field phase (no field applied), it will slip back to phases where the field is accelerating, but at the same time it will be chirped and compressed. The key point is that compression and acceleration take place at the same time within the same linac section, actually the first section following the gun, that typically accelerates the beam, under these conditions, from a few MeV ( $> 4$ ) up to 25-35 MeV.

Therefore, the name *velocity bunching* refers to a correlation between particle velocity and position (phase) within the bunch, opposed to the magnetic compression technique which relies on a correlation between particle path length through the device and particle position (phase) within the bunch; since the chicane performing magnetic compression is often named *magnetic compressor*, the linac section performing *velocity bunching* is often named *RF (bunch) compressor* and velocity bunching itself is sometimes named *RF (bunch) compression*.

We show here how this method can preserve the low transverse emittance achieved at the exit of the photo-injector, reaching at the same time peak currents comparable with those produced by magnetic compressors.

The theoretical model explaining velocity bunching is based on a Hamiltonian treatment as follows. The interaction of a beam with a RF wave given by  $E_z = E_0 \sin(\omega t - kz + \phi_0)$  is described by the Hamiltonian

$$H = \frac{1}{2} \frac{p_r^2}{\gamma_r} + \sqrt{1 - \frac{1}{\gamma_r^2}} \cos(\omega t - kz + \phi_0) \quad (24)$$

where  $\frac{1}{\gamma_r}$  is the normalized electron energy,  $\phi = kz - \omega t + \phi_0$  is its phase with respect to the wave, while  $\frac{1}{\gamma_r} = eE_0/mc^2 k$  is the dimensionless vector potential amplitude and  $\gamma_r = 1/\sqrt{1 - \frac{1}{\gamma_r^2}}$  is the resonant gamma of the wave (conventional traveling wave structures operate at  $\gamma_r = 1$ ,  $k = \omega/c$ ).

A wave whose phase velocity is slightly smaller than  $c$ , so that  $k = \omega/c + \Delta k$ , is characterized by  $\gamma_r = 1/\sqrt{1 - \frac{1}{\gamma_r^2}}$ ,  $\Delta k = \sqrt{1 - \frac{1}{\gamma_r^2}}/2c$  (assuming  $c\Delta k/\omega \ll 1$ ).

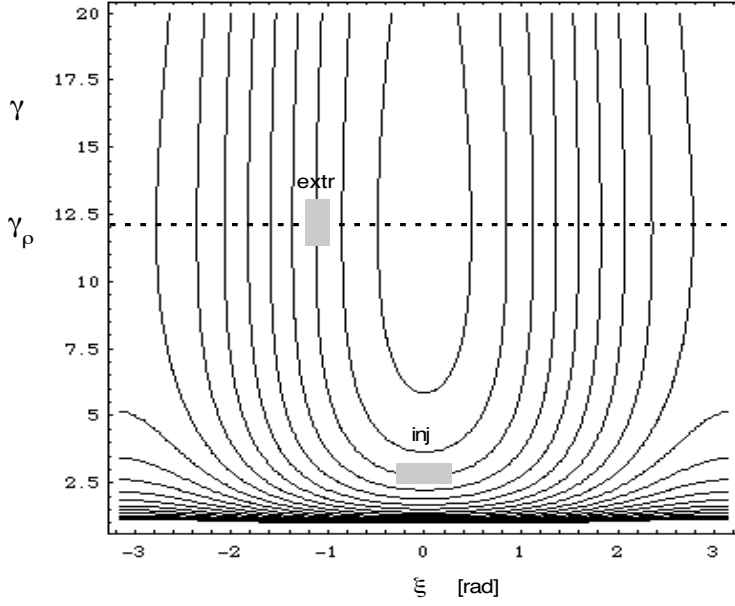


**FIG. 15:** Phase space plots of a slow RF wave ( $\beta_r$  finite) showing the basics of phase compression in a linac

The basic mechanism underlying the rectilinear compression effect is illustrated in Fig.15, where the contour lines of the Hamiltonian associated to a slow RF wave having  $\beta_r = 12$  (*i.e.*  $\beta_r = 0.9965$  and  $\beta_k = 0.0035 \beta/c$ ) and  $\beta = 0.2$  are plotted. If the bunch is injected into the wave at zero phase (*i.e.* when the field of the wave is not accelerating), at an energy lower than the synchronous one (which corresponds to  $\beta$ ), it will slip back in phase and go up in energy, being accelerated by the wave). By extracting the beam from the wave at the time it reaches the resonant  $\beta$ , *i.e.* when it becomes synchronous with the wave, we make the bunch undergo one quarter of synchrotron oscillation. In doing so, the beam is compressed in phase as depicted in Figure 15.

**TAB. 1:** Resonant gamma factors and corresponding phase velocities and wave number shifts.

$\beta_r$	$\beta_r$	$\beta k$
20	0.9987	0.0013
35	0.9996	0.0004
60	0.99986	0.00014
infinite	1	0

The compression ratio has been calculated elsewhere [5] to be:

$$C = 2\beta_0 |\sin \bar{\beta}_{ex}| \sqrt{\beta_0^4 + \frac{1}{\beta_b} \frac{\beta_b^2}{\beta_b}} \quad (25)$$

where  $\beta_0$  and  $\beta_b/\beta_b$  are the initial phase spread and energy spread of the bunch ( $\bar{\beta}_{ex}$  is

the average beam exit phase at  $\varphi = \varphi_f$ ).

This expression gives a good first order estimate of the compression for an uncorrelated longitudinal phase space distribution at injection. The actual beam produced by photo-injectors has energy-phase correlations given by space charge and RF effects, so that the best performances of a rectilinear RF compressor may occur for extraction of the beam from the wave at energies different than  $\varphi_f$  (as shown in the following), and can be enhanced with a longitudinal emittance compensation scheme, through use of a higher harmonic cavity to correct RF induced non linear energy spread.

In order to preserve the beam transverse emittance we have to integrate the longitudinal dynamics of the RF compressor into the process of emittance compensation, which is achieved for a beam at constant current by matching it on the invariant envelope. The analytical model is basically an extension of the invariant envelope theory [3], to the case of currents growing together with energy along the RF compressor. The analysis reported in the previous section is valid only for beams carrying constant peak current  $I$ , as usual in photoinjectors when no compression mechanism is applied (or space charge debunching is negligible). In order to extend the model to the case of RF compression (where  $I$  grows by a large factor) we have assumed that the current grows in the compressor at the same rate as the energy, i.e.  $I = \frac{I_0 \varphi}{\varphi_b}$ , where  $I_0$  and  $\varphi_b$  are the initial values for the current and the energy, respectively, at injection into the compressor. This assumption is derived by observations performed in several simulations of the RF compressor, indicating that best results in terms of final beam brightness are achieved under this condition, which indeed gives rise to a new beam equilibrium. It should be noted that this condition may be violated strongly near the end of the compression process, but as this occurs at high energy, the violation may not have serious consequences.

In fact, the rms envelope equation becomes in this case,

$$\varphi'' + \varphi' \frac{\varphi''}{\varphi'} + \varphi \frac{\varphi''^2 \varphi'^2}{\varphi^2} - \frac{I_0}{2I_A \varphi \varphi_b \varphi^2} = 0, \quad (26)$$

whose new exact analytical solution is

$$\varphi_{RFC} = \frac{I}{\varphi \varphi_b} \sqrt{\frac{I_0}{2I_A \varphi_b}}, \quad (27)$$

*i.e.* a beam flow at constant envelope (instead of  $I/\sqrt{\varphi}$  as for the invariant envelope). This is dictated by a new equilibrium between the space charge defocusing term (decreasing now as  $I/\varphi^2$ ) and the focusing and acceleration terms (imparting restoring forces to the beam): while for the invariant envelope equilibrium is achieved even in absence of external focusing, *i.e.* at  $\varphi = 0$ , in this case we need to provide external focusing.

Just for sake of comparison we notice that the solution for Brillouin flow (drifting beam at constant energy and constant current undergoing a rigid rotation in the solenoid field  $B_{sol}$ )

becomes  $\sigma_{BRI}^{BAC} = \frac{mc}{eB_0} \sqrt{\frac{I_0}{2I_A \sigma_b}}$  in the case of current increasing linearly along the drift

( $I = (\sqrt{k}z)I_0$ ) for a corresponding growing solenoid field of the type  $B_{sol} = \sqrt{\sqrt{k}z}B_0$  (also in this case we obtain a constant envelope matched beam through the system, like for the case of RF compression). The beam size  $\sigma_{BRI}^{BAC}$  describes what typically is found in ballistic bunching to the beam envelope, which needs to be controlled by providing a ramped solenoid field to avoid envelope instability in this envelope dynamics.

What is relevant for the emittance correction process is the behavior of the envelope and associated emittance oscillations due to envelope mismatches at injection. Let us assume that the injecting envelope is mismatched with respect to the equilibrium condition such that  $\sigma_{INV0} = \sigma_{INV} \sigma \sigma_0$ , or  $\sigma_{RFC0} = \sigma_{RFC} \sigma \sigma_0$ , or  $\sigma_{BRI0}^{BAC} = \sigma_{BRI}^{BAC} \sigma \sigma_0$ , depending on the type of equilibrium flow that the beam has to be matched on. A perturbative linear analysis of the rms envelope equations given above brings to these solutions for the envelope mismatches:

$$\sigma_{INV} = \sigma_{INV0} \cos \left[ \sqrt{\frac{I}{4} + 2\sigma^2} \ln \frac{\sigma \sigma_0}{\sigma_b} \right] + \sigma_0 \left[ \quad \right] \quad (28)$$

for the invariant envelope,

$$\sigma_{RFC} = \sigma_{RFC0} \cos \left[ \frac{I}{\sigma} \ln \frac{\sigma \sigma_0}{\sigma_b} \right] + \sigma_0 \left[ \quad \right] \quad (29)$$

for its generalization in RF compressors, and

$$\sigma_{BRI}^{BAC} = \sigma_{BRI0}^{BAC} \cos \left[ \frac{eB_0 \sqrt{\sqrt{k}z}}{mc \sigma} \ln \frac{\sigma \sigma_0}{\sigma_b} \right] + \sigma_0 \left[ \quad \right] \quad (30)$$

for the ballistic bunching case.

These envelope mismatches produce emittance oscillations in laminar beams because of the spread in initial mismatches due to different slice currents [3]. The emittance behaviors for the three flow conditions turn out to be:

$$\sigma_h^{INV}(z) \approx \sqrt{\sigma_{bff}^2 + \frac{I \langle \sigma_{INV}^2 \rangle}{\frac{I}{4} + 2\sigma^2}} \quad , \quad (31)$$

$$\sigma_h^{RFC}(z) \approx \sqrt{\sigma_{bff}^2 + \frac{I_0 \langle \sigma_{RFC}^2 \rangle}{\sigma^2 \sigma_b}} \quad , \quad \text{and} \quad (32)$$

$$\epsilon_t^{BAC}(z) \propto \sqrt{\epsilon_{eff}^2 + \frac{I_0 \left\langle \epsilon_{BRI0}^{BAC^2} \cos^2 \left[ \frac{eB_0 \sqrt{\epsilon_k}}{mc\beta} z + \epsilon_0 \right] \right\rangle}{B_0^2 \epsilon_b}}, \quad (33)$$

where the average  $\langle \epsilon \rangle$  is performed over the initial spread of mismatches in different bunch slices and  $\epsilon_{eff}$  accounts for the non linear and thermal contributions.

While the rms normalized emittance oscillates and adiabatically damps as  $\epsilon^{1/2}$  in the invariant envelope case ( $\epsilon_t^{INV}$ , constant current), it oscillates at constant amplitude along the RF compressor ( $\epsilon_t^{RFC}$ ), and with a frequency scaling similar to the invariant envelope case, *i.e.*

$$\frac{\epsilon}{z} \ln \left[ 1 + \frac{\epsilon_k}{\epsilon_b} \right], \text{ as compared with } \frac{\sqrt{1/4 + 2\epsilon^2}}{z} \ln \left[ 1 + \frac{\epsilon_k}{\epsilon_b} \right].$$

In the case of ballistic bunching the emittance  $\epsilon_t^{BAC}$  exhibits on the other hand a completely different scaling, with constant amplitude

$$\text{but an increasing frequency, as } \frac{eB_0 \sqrt{\epsilon_k}}{mc\beta}.$$

This is the basis how the transverse emittance can be corrected in the RF compressor; by connecting the two types of flow carefully (proper matching) we can make the emittance oscillate at constant amplitude in the RF compressor and smoothly connect these oscillations to a damped oscillatory behavior in the accelerating sections following the RF compressor, where the beam is propagated under standard invariant envelope conditions - this is possible because of the similar frequency behavior of the two flows.

A possible limitation can occur in all cases, which is due to the requirement of additional external focusing that, as discussed in the previous section, can drive a plasma frequency spread due to chromatic effects.

As an example the SPARC photoinjector [19] design assumes a 1.6-cell S-band RF gun of the BNL/SLAC.UCLA type equipped with an emittance compensating solenoid and followed by three standard SLAC 3-m TW sections, each embedded in a solenoid. The preliminary results of the first simulations show that with a proper setting of accelerating section phases and solenoid strengths it is possible, applying the compression method described above, to increase the peak current while preserving the beam transverse emittance. An optimized parameter set is shown in Table 2.

**TAB. 2:** RF compressor parameters

TW Section	I	II	III
Gradient (MV/m)	15	25	25
Phase (Deg)	-88.5	-64.3	0 (on crest)
Solenoid field (Gauss)	1120	1400	0

In order to obtain slow bunching of the beam (the current grows about at the same rate of the energy) and to increase the focusing magnetic field with the current during the compression process, we used the first two sections as compressor stages.

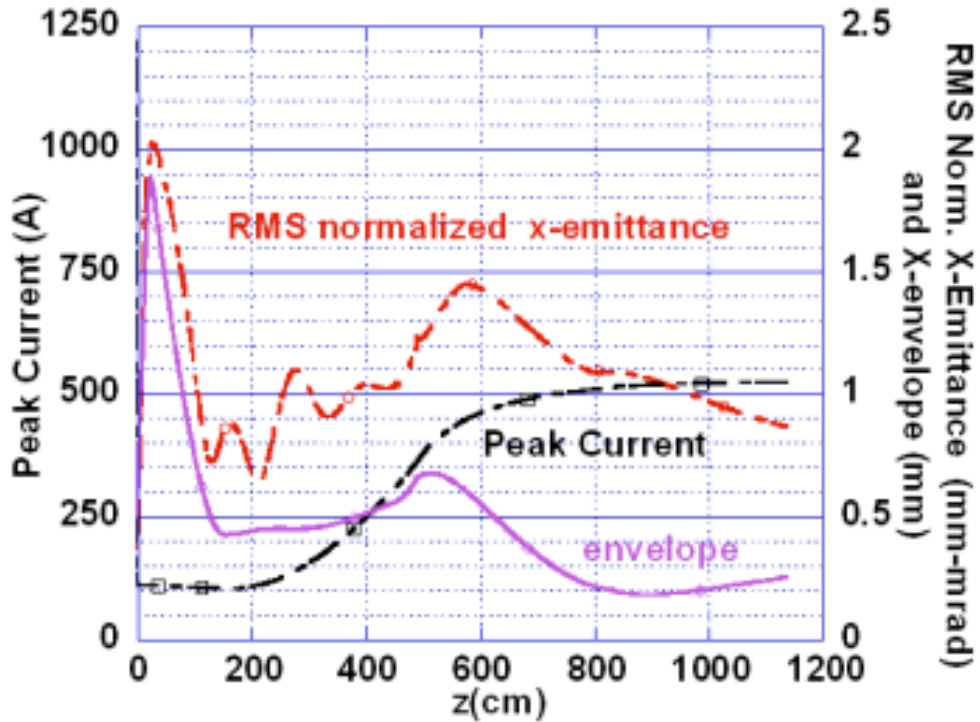


**FIG. 16:** RMS normalized emittance, beam envelope and peak current vs the distance from the cathode.

The plots in Fig. 16, of the peak current and the transverse normalized rms emittance (a thermal emittance of 0.3 mm mrad is included) as a function of the distance from the cathode computed by PARMELA for 10K particles, show that a peak current of 510 A can be reached with a transverse rms normalized emittance of 0.9  $\mu\text{m}$ . The final beam energy is only 120 MeV, so additional care must still be taken after this point in order to properly damp residual emittance oscillation driven by space charge correlations.

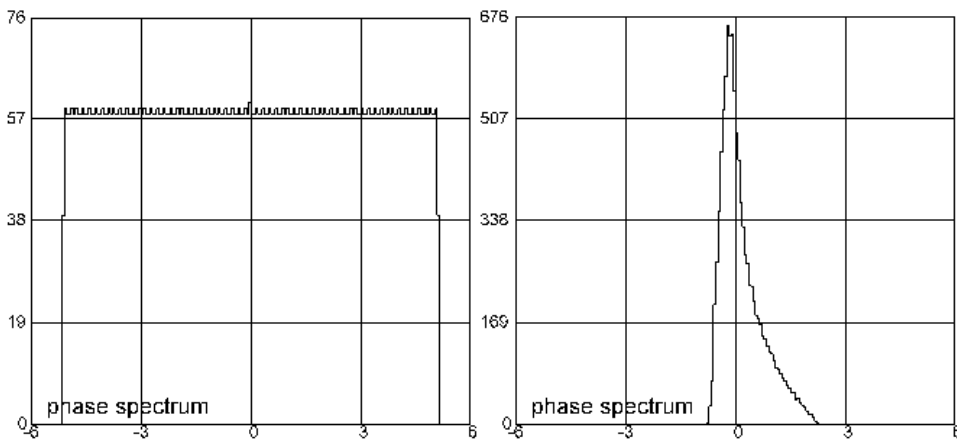


**FIG. 17:** initial and final phase spectrum.

The plots in Figures 17 and 18 show the evolution of the bunch during the compression as derived from PARMELA computations. One can see that the bunch temporal distribution that is

uniform at the beginning tends to a triangular shape: so the value of the peak current in the plot of Fig. 16, that is simply scaled with the rms bunch length, in reality is an average current in the bunch corresponding to a larger value in the peak (almost double with respect to the average).

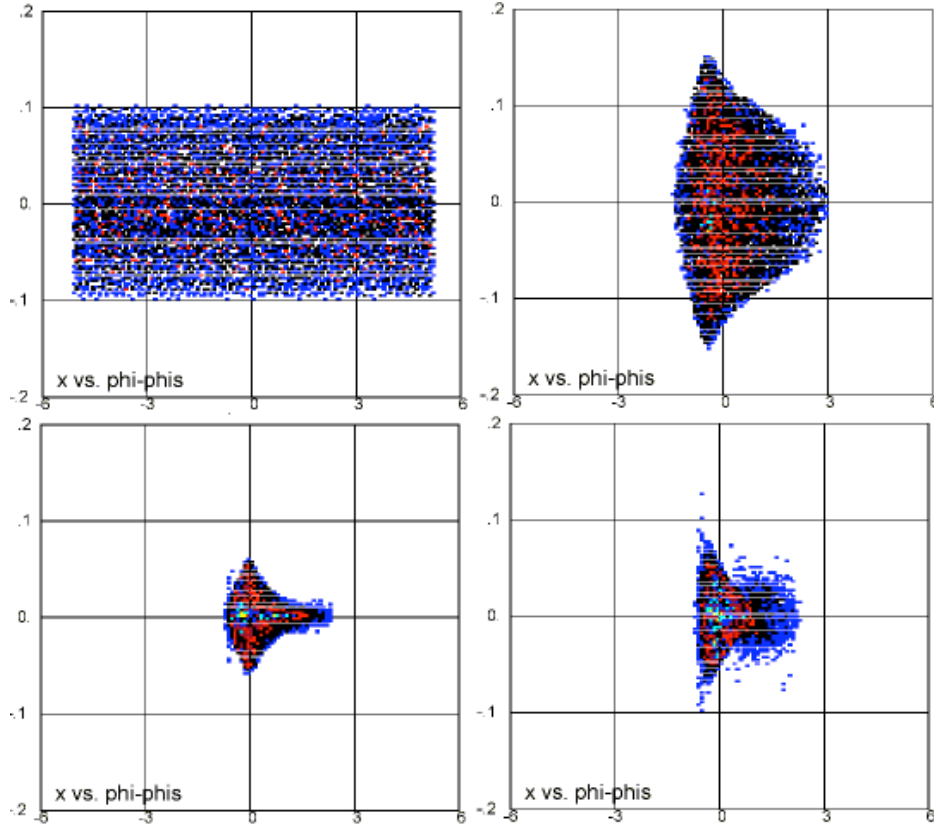


**FIG. 18:**  $x$ - $\phi$  plots: Top, left plot: initial RF gun, top, right plot: output Section 1; bottom, right plot, output Section 2; bottom left plot: output Section 3.

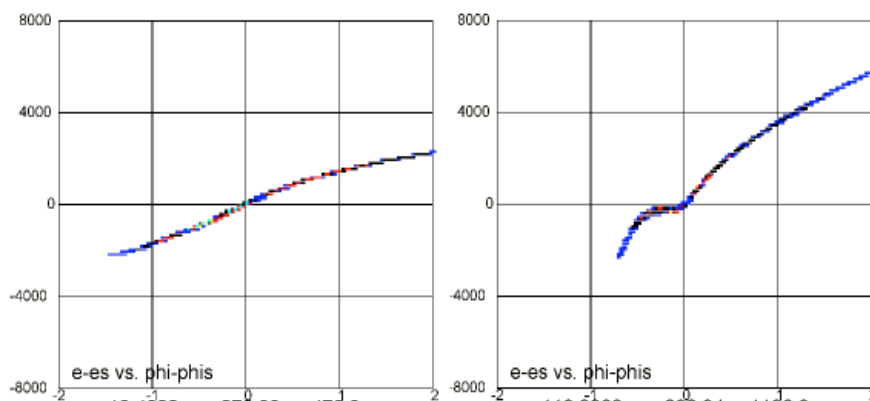


**FIG. 19:** Energy-phase space: left: output Section 1  $I=330$  A, left: output Section 3  $I=510$  A.

From the point of view of the beam transverse dynamics, during the compression slices with different longitudinal position within the bunch experience different net focusing strengths. In particular the head of the bunch, which contains the maximum charge is defocused, while the tail tends to be focused or overfocused, as is shown in Figure 18, which displays the plot  $x$ - $\phi$  at different points of the compressor line.

According to PARMELA convention in the plots of Figures 18 and 19 the head of the bunch is on the left. From the point of view of the longitudinal phase space, as it can be seen in Figure 19, when the current becomes greater than 400 A the bunch head tends to loose the energy-phase correlation differently from the tail that contains less charge, which could be a problem for a further compression of the bunch at higher energy. This point will be investigated more carefully in the future.

The first experimental evidence of RF compression was reported by the BNL-ATF group [24], which observed a relevant reduction of the electron bunch length with respect to the laser pulse length illuminating the photocathode, whenever the launch phase at the cathode close to 0 (low, but increasing, electric field) was used. Extracting 40 pC with a 4 ps rms laser pulse, they measured 370 fs electron bunches at the exit of the second linac section (52 MeV) with an rms normalized emittance of 0.5  $\mu\text{m}$ . Comparing these results to simulations, they inferred a bunch length of 1.6 ps at the gun exit, 0.63 ps at the end of the drift space between the gun and the first linac, and 0.37 ps at the exit of the entire system. Clearly the type of bunching process applied was mixed: velocity bunching in the gun, ballistic bunching in the drift and velocity bunching again in the linac. This last, anyway, was the smallest contribution and this explains the rather large emittance measured for the corresponding bunch charge.

It is interesting to note that the same authors recently proposed to repeat that experiment by decreasing the amount of bunching achieved in the drift and increasing the velocity bunching applied in the linac [25]. Simulations reported in this reference show that a 25 pC bunch can be extracted by launching a 4 ps laser pulse onto the cathode, to obtain a 1 ps electron bunch at the gun exit and a 15 fs bunch length at the exit of the second linac (almost no compression performed in the drift space). It is also interesting that the final value for the emittance is 1  $\mu\text{m}$  in case of no additional focusing applied around the linac sections, while 0.5  $\mu\text{m}$  can be achieved if a solenoid is located in the middle of the first linac section. This is the location where most of the velocity bunching is done, and the solenoid is used to control the beam envelope, thus confirming the theoretical predictions [25].

The first experiment dedicated to verify the velocity bunching concept was performed at UCLA PBPL [6], unfortunately in a photo-injector lay-out (Neptune Laboratory injector) that is clearly not optimized to perform RF compression. Indeed, the first linac section after the gun is a short (0.6 m) PWT linac, not long enough to perform a substantial acceleration together with bunching, *i.e.* to allow the bunch to slip back in phase with respect to the RF wave. However, they measured a 0.39 ps bunch length after the linac by using coherent transition radiation autocorrelator signal, and they reconstructed by simulations the beam dynamics to show that the bunching was still a mixed one, velocity bunching in the PWT linac and ballistic in the following drift.

An experiment performed recently with a photoinjector system operating long TW linac sections after the gun was done at the BNL-DUVFEL laboratory [7]. Here they excited the photocathode with a 1.15 ps laser pulse length extracting 200 pC of bunch charge, reaching a minimum 0.5 ps bunch length at the exit of the photoinjector system, at a beam energy of 55 MeV (no compression was performed in the gun neither in the drift space). No further compression could be applied to go below 0.5 ps because of lack of additional focusing: the beam envelope could not be controlled. The excellent agreement found in this experiment

between simulations and experimental measurements, shown in Fig. 20, once again provides a nice confirmation that this technique is very promising in attaining fs electron bunches at high brightness. As a latest news, an ongoing experiment at the Livermore PLEIADES lab by a UCLA/LLNL team, is producing outstanding results both in terms of minimum bunch length (0.33 ps) and emittance achieved. Work is in progress, with quite good perspectives [8].

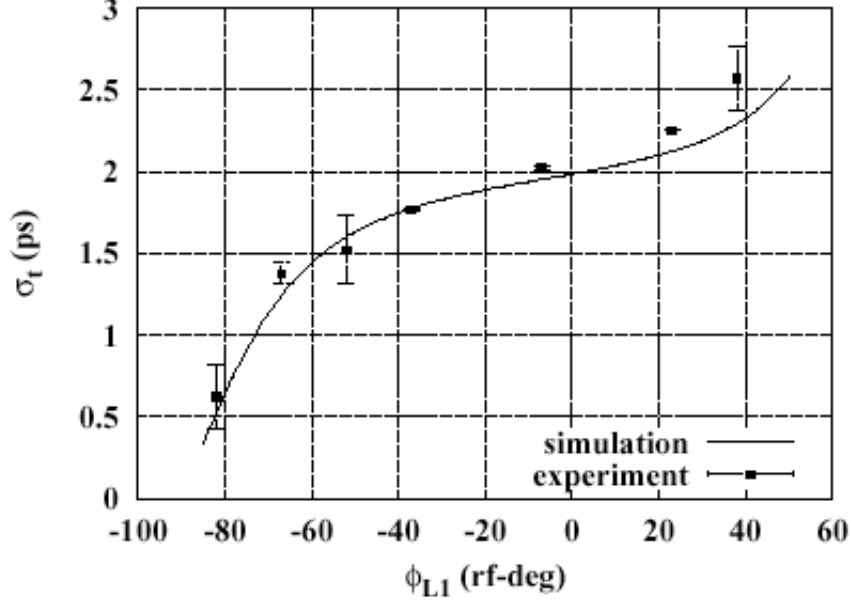


**FIG. 20:** rms bunch length as a function of the phase of the first linac section.

As a conclusion, a fully optimized dedicated photo-injector for application of the velocity bunching technique still does not exist: one of the missions of the SPARC project is indeed to design and commission such a system [19]. The full potential of such a technique has yet to be explored experimentally; high brightness, femtosecond-class bunches may be reached after a full exploitation this scheme.

#### 4 FLAT BEAMS PRODUCTION: THE CONCEPT OF EMITTANCE EXCHANGE

In the context of electron-positron linear collider (LC) projects, the goals of electron sources are even more challenging. Linear colliders in fact require high charge, polarized electron beams with extremely low normalized emittances, with geometric average  $\sqrt{\epsilon_{tx} \cdot \epsilon_{ty}} \approx 10^{-1}$  nm [26]. The recent analytical and numerical efforts in understanding beam dynamics in RF photo-injectors have again raised the question whether the performance of an RF electron gun based injector could be competitive with respect to a damping ring. A possible answer to this question is discussed in this section.

In terms of colliding beam parameters the luminosity in a LC is defined as

$$L = \frac{n_b N_e^2 f_{rep}}{4 \epsilon_{tx}^* \epsilon_{ty}^*} H_D = \frac{P_b}{E_{cm}} \frac{N_e}{4 \epsilon_{tx}^* \epsilon_{ty}^*} H_D , \quad (34)$$

where  $P_b = E_{cm} n_b N f_{rep}$  is the beam power,  $E_{cm}$  the center of mass energy,  $n_b$  the number of bunches per pulse,  $N_e$  the number of electron (positron) per bunch,  $f_{rep}$  the pulse repetition frequency,  $\sigma_{x,y}^*$  the horizontal (vertical) beam size at the interaction point (IP), and  $H_D$  the beam-beam disruption enhancement factor [27].

A primary effect of the beam-beam interaction is an enhancement of the luminosity due to the pinch effect, *i.e.* the reduction of the of the cross section of both beams, occuring at the IP that is included in the luminosity definition through the factor  $H_D \geq 1$ . When electron and positron beams are intersecting, the defocusing electrostatic force diminishes by mutual space charge neutralization and only the focusing magnetic force plays a role, as a strong attractive transverse force between two opposite currents; both particle species are deflected towards the axis as in a focusing lens. The benefit of luminosity enhancement is reduced by the fact that particles emit synchrotron radiation in the strong electromagnetic fields of the opposite bunch, known as "beamstrahlung". The probability that a given particle will experience a significant energy loss before colliding with another particle in the opposite beam becomes high. The average fractional beam energy loss is approximately given by

$$\Delta_E = \frac{r_e^3 N_e^2 \sigma_z}{\sigma_z (\sigma_x^* + \sigma_y^*)^2}. \quad (35)$$

Beamstrahlung leads to a large spread in the center of mass energies, reducing the accuracy during the measurement of a specific event,  $\Delta_E$  therefore has to be limited typically to a few percent. By choosing a large beam aspect ratio  $\sigma_x^* \gg \sigma_y^*$ ,  $\Delta_E$  becomes independent from the vertical beam size and luminosity can be increased by making  $\sigma_y^* \sqrt{\sigma_{h,y} \sigma_y^*} / \sigma_z$  as small as possible. Choosing  $\sigma_y^* = \sigma_z$  the luminosity can be expressed eliminating  $N_e$  as

$$L = \frac{P_b}{E_{cm}} \sigma_z \sqrt{\frac{\Delta_E}{\sigma_{h,y}}} \sigma_z H_D. \quad (36)$$

An injector for a linear collider must provide a flat beam in order to reduce beamstrahlung effects at the interaction point (IP), thus implying  $\sigma_{h,y} \ll \sigma_{h,x}$ . But a production of a flat beam directly from the cathode surface would increase the difficulties for emittance compensation, easily achieved by means of a symmetric solenoid as discussed in the previous section. A flat beam is typically delivered by a damping ring. Nevertheless a transformation of a round beam derived from a photoinjector into a flat beam has been recently proposed [28] by means of simple linear beam optics adapter at the exit of a injector.

This transformation is possible with a magnetized beam, as produced by an rf gun with a cathode embedded in a solenoid field [9]. At the exit of the gun/solenoid system the beam has an angular momentum given by

$$p_{\perp} = \frac{1}{2} e B_{z,c} R_c^2, \quad (37)$$

where  $B_{z,c}$  is the on cathode magnetic field, and  $R_c$  the laser spot radius. Both transverse planes are thus coupled by the beam rotation. Such rotation can be arrested by a suitable choice of a skew quadrupole triplet that, in addition, changes the emittance ratio according to the relation,

$$\frac{\epsilon_x}{\epsilon_y} = 1 + \frac{2\epsilon_r^2}{\epsilon^2 \epsilon_r'^2}, \quad (38)$$

for a beam with rms size  $\epsilon_r$  and rms angular spread  $\epsilon_r'$ . The final emittance ratio is thus simply variable by adjusting the free parameter  $\epsilon = 2p_o/eB_{z,c}$ , via the magnetic field on the cathode. Design studies based on this scheme [9] show that for a 0.8 nC charge one can obtain  $\epsilon_{ix}=1.1 \times 10^{-5}$  m and  $\epsilon_{iy}=3 \times 10^{-8}$  m, with an emittance ratio of about 370. Additional studies are under way for a better understanding of the space charge effects when the transformation is applied at low energy. A first successful demonstration of this method was recently achieved at the A0 experiment at FNAL [29].

In Fig. 21 the beam image downstream the quadrupole triplet in the A0 experiment is shown, and it has been verified that the beam remains flat as it drifts farther downstream, an important experimental achievement that demonstrate the effectiveness of the linear beam optics adapter in the context of RF photoinjector. The measured ratio of emittances is about 50, with  $\epsilon_{ix}=0.9$   $\mu$ m and  $\epsilon_{iy}=45$   $\mu$ m for a 1 nC beam, which yields a geometric mean emittance that is still rather high at 6.5  $\mu$ m. Additional experiments are foreseen in the near future to optimize the emittance compensation process.

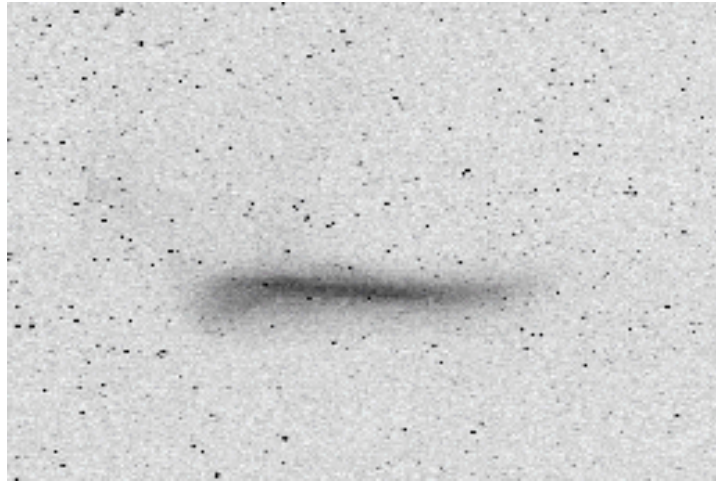


**FIG. 21:** Beam profile on OTR screen 1.2 m downstream of the third skew quadrupole at FNAL A0 flat beam experiment.

## 5 ACKNOWLEDGEMENTS

We like to thank W. Decking, H. Edwards, D. Edwards, P. Emma, K. Floettmann, W. S. Graves, K. J. Kim, P. Musumeci, D. T. Palmer, Ph. Piot, V. Telnov, X. J. Wang, for the many

helpful discussions and suggestions.

## 6 REFERENCES

- [1] Linac Coherent Light Source (LCLS) Conceptual Design Report, SLAC-R-593 (2002).
- [2] TESLA XFEL, Technical Design Report (Supplement), DESY 2002-167, TESLA-FEL 2002-09, (2002).
- [3] L. Serafini, J. B. Rosenzweig, "Envelope analysis of intense relativistic quasilaminar beams in rf photoinjectors: a theory of emittance compensation", *Phys. Rev. E* **55** (1997) 7565.
- [4] P. Emma, "Accelerator physics challenges of X-rays FEL SASE sources", *Proc. Of EPAC-02*, Paris 2002.
- [5] L. Serafini, M. Ferrario, "Velocity Bunching in PhotoInjectors" , *AIP CP* 581, 2001, pag.87.
- [6] P.Musumeci, R.J.England, M.C.Thompson, R.Yoder, J.B.Rosenzweig, "Velocity Bunching Experiment at the Neptune Laboratory", these proceedings.
- [7] P. Piot, L. Carr, W. S. Graves, and H. Loos, "Subpicosecond compression by velocity bunching in a photoinjector", these proceedings.
- [8] G. Le Sage et al., "Ultrafast Materials Probing with the LLNL Thomson X-ray source", these proceedings.
- [9] R. Brinkmann, Y. Derbenev, and K. Flöttmann "A low emittance, flat-beam electron source for linear colliders", *Phys. Rev. ST Accel. Beams* 4, 053501 (2001)
- [10] K. Bishofberger et al., "Flat Electron Beam Production at FNAL - A Status Report", *Proc. Of LINAC 2002*, Korea.
- [11] C. A. Brau, "What Brightness Means", these proceedings.
- [12] J. Rossbach, E. L. Saldin, E. A. Schneidmiller, M. V. Yurkov, "Interdependence of Parameters of an X-ray FEL", TESLA-FEL 95-06.
- [13] Linac Coherent Light Source (LCLS) Conceptual Design Report, SLAC-R-593 (2002)
- [14] M. Reiser, "Theory and Design of Charged Particle Beams", J. Wiley & Sons, (1994).
- [15] PH. Piot, "Review of experimental results on high brightness electron beams sources", these proceedings.
- [16] J. Rosenzweig and L. Serafini, "Transverse particle motion in radio-frequency linear accelerators", *Phys. Rev. E* 49 (1994) 1599.
- [17] B. E. Carlsten, *Nucl. Instrum. Methods A* **285**, 313 (1989).
- [18] S. G. Anderson and J. B. Rosenzweig, "Non-equilibrium transverse motion and emittance growth in ultra-relativistic space-charge dominated beams, *Phys. Rev. ST Accel. Beams* 3(9), 094201 , (2000).
- [19] L. Serafini, "New perspectives and programs in Italy for advanced applications of high brightness beams", these proceedings.
- [20] J. Clendenin et al., "Reduction of thermal emittance of rf guns", SLAC-PUB-8284 (1999)
- [21] M. Ferrario et al., "HOMDYN Study For The LCLS RF Photo-Injector" *Proc. of the 2<sup>nd</sup> ICFA Adv. Acc. Workshop on "The Physics of High Brightness Beams"*, UCLA, Nov., 1999, see also SLAC-PUB-8400.
- [22] J. Buon, "Beam phase space and emittance", in CERN 94-01.
- [23] J. B. Rosenzweig and E. Colby, Charge and Wavelength Scaling of RF photoinjector design, TESLA-95-04.
- [24] X.J. Wang et al, *Phys. Rev. E* 54, R3121 (1996).

- [25] X.J. Wang and X.Y. Chang, *Femto-seconds Kilo-Ampere Electron Beam Generation*, in publ. in the Proc. of FEL 2002 Conf.
- [26] V. Telnov, Physics goals and parameters of photon colliders, Proc. of II Workshop on e-e- interaction at TeV Energies, To be published in Int. J. Mod. Phys. A.
- [27] K. Yokoya, *Beam-Beam Interaction in Linear Collider*, Proc. Joint USA/CERN/JP/Ru Acc. Sch. High Quality Beams, AIP 592 (2000).
- [28] Ya Derbenev, Adapting Optics for High Energy Electron Collider, UM-HE-98-04, Univ. Of Michigan, 1998.
- [29] D. Edwards et al., The flat beam experiment at the FNAL photoinjector, Proc. of LINAC 2000, Monterey.